Materials Chemistry and Physics 291 (2022) 126645

Contents lists available at ScienceDirect

Materials Chemistry and Physics

journal homepage: www.elsevier.com/locate/matchemphys

Signature of adsorbed solvents for molecular electronics revealed via scanning tunneling microscopy

Tamara de Ara [a], Carlos Sabater [a,*], Carla Borja-Espinosa [b,a], Patricia Ferrer-Alcaraz [a], Bianca C. Baciu [c], Albert Guijarro [c], Carlos Untiedt [a]

[a] Departamento de Física Aplicada and Unidad asociada CSIC, Universidad de Alicante, Campus de San Vicente del Raspeig, E-03690, Alicante, Spain
[b] Yachay Tech University, School of Physical Sciences and Nanotechnology, 100119, Urcuquí, Ecuador
[c] Departamento de Química Orgánica and Instituto Universitario de Síntesis Orgánica, Universidad de Alicante, Campus de San Vicente del Raspeig, E-03690, Alicante, Spain

HIGHLIGHTS

- Benzene, cyclohexane, and toluene as organic solvents for molecular electronics at ambient conditions.
- Organic solvents remain physisorbed on gold surfaces after a controlled evaporation process.
- STM and STM-BJ experiments demonstrate the presence of organic solvent molecules on gold surfaces at ambient conditions.
- Direct measurements of the diameter and electronic transport in single organic molecules of benzene, cyclohexane, and toluene.
- The contribution of the organic solvents cannot be neglected in molecular electronic transport measurements.

GRAPHICAL ABSTRACT

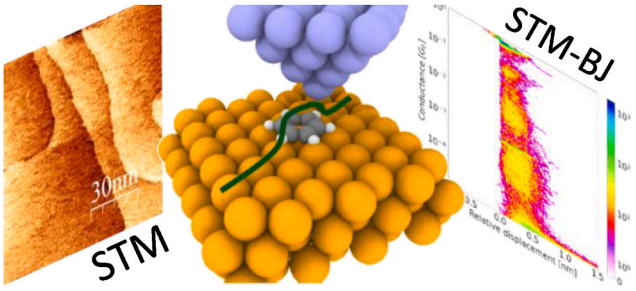

ARTICLE INFO

Keywords:
Molecular electronics
STM
Electronic transport
Organic solvents
Absorbed molecules
Break-junction

ABSTRACT

After evaporation of the organic solvents, benzene, toluene, and cyclohexane on gold substrates, Scanning Tunneling Microscope (STM) shows the presence of a remaining adsorbed layer. The different solvent molecules were individually observed at ambient conditions, and their electronic transport properties characterized through the STM in the Break Junction approach. The combination of both techniques reveals, on one hand, that solvents are not fully evaporated over the gold electrode and, secondly, characterize the electronic transport of the solvents in molecular electronics.

1. Introduction

Organic solvents such as benzene, toluene or cyclohexane are commonly used for the preparation of clean surfaces or for the deposition of other molecules [1]. These apolar solvents are used under the believe that they can be easily removed through thermal evaporation,

* Corresponding author.
E-mail address: carlos.sabater@ua.es (C. Sabater).

https://doi.org/10.1016/j.matchemphys.2022.126645
Received 23 May 2022; Received in revised form 5 August 2022; Accepted 6 August 2022
Available online 17 August 2022
0254-0584/© 2022 The Authors. Published by Elsevier B.V. This is an open access article under the CC BY-NC-ND license (http://creativecommons.org/licenses/by-nc-nd/4.0/).

their contribution during the electrical transport measurement experiments should be negligible [1,2] or that these may be distinguishable from the target molecules in the solution [3]. The understanding of the role of the solvents in the study of single molecular transport should be improved, despite all the advances of the area during the last decades [4–9].

In this respect, the single metal-molecule-metal junction constitutes the basic building block for molecular electronics. Many different molecules at different environmental conditions, from cryogenic [5,10–13] to ambient conditions [14–18], have been studied through the years. Contrary to the low temperature strategy, the study of molecular junctions at ambient conditions normally has made use of functional groups [19] attached to the molecule periphery, in order to help in the anchoring to the electrodes [20]. Usually a thiol [18,21–24] group is used to enhance and strengthen the affinity. A paradigmatic example of these differences in strategies is the case of the study of the benzene molecule (C_6H_6). While at low temperatures different studies have been performed on the bare molecule [10,25,26], for ambient conditions the molecule has been functionalized, as it was commonly believed that otherwise the molecule would not remain anchored to the electrodes [21–23]. However, it is well known that a monolayer of non-functionalized molecules can bind to clean surfaces and be physisorbed by van der Waals forces. These forces may be strong enough to perform electronic transport measurements at ambient conditions, what constitute the starting hypothesis in our study. In this work, we study the effect of physisorption on gold of different bare molecules often used as organic solvents in molecular electronics: benzene (C_6H_6), cyclohexane (C_6H_{12}) and toluene ($C_6H_5CH_3$). The presence of these molecules on the surfaces is characterized using a Scanning Tunneling Microscope [27] (STM), and their typical conductance fingerprint through STM-based Break-Junction (STM-BJ) experiments [14], both operated at ambient conditions (see Fig. 1 illustration (a) and (b)). These experiments, not only allow to identify the presence of the molecules, they also allow to measure, on one side, the height profile of isolated molecules. Fig. 1 panel (c) shows an experimental STM profile of benzene on a gold substrate, following the procedure depicted in the illustration of panel (a) and, on the other side, panel (d) shows the evolution of the conductance while stretching the molecular junction as shown in panel (b).

2. Methods and material

For the experiments a freshly distilled, pre-purified solvent (or compound) was employed for every experiment (details in the purification process at sup. inf. section). These high purity solvents, benzene (> 99.95 %), cyclohexane (> 99.98 %) and toluene (> 99.95 %) were stored in borosilicate glass containers.

Our investigation was performed using two different experimental setups. In our STM-BJ experiments, for recording full conductance traces across six orders of magnitude, a three stages current-voltage amplifier was designed and built with gains 10^6, 10^8 and 10^9 V/A. These three output channels are merged via software. After merging the signals, we subtract the saturation of the amplifier of high gain (details in sup. inf.).

In the case of STM-BJ experiments, the tips and surface electrode were formed by two gold wires (0.5 mm, GoodFellow, 99.999% [28]) facing the curved cylindrical surfaces one against the other in a perpendicular configuration. On the other side, for topographic images, we used an STM with a $Pt_{90}Ir_{10}$ tip (0.25 mm, GoodFellow [28]). Moreover, we used gold substrates from Arrandee [29] for these experiments.

For STM experiments, substrates were embedded in piranha solution in a ratio 3:1 of sulfuric acid and hydrogen peroxide to clean the surface. Later, for removing the piranha solution, the samples are immersed in miliQ water. A flame annealing process is performed to acquire flat gold. Imaging of the surface is carried out as to ascertain the cleanness and formation of the (111) terraces of gold with no traces of adsorbed molecules. It should be pointed out that in our images the herringbone reconstruction [30] is clearly seen indicating the cleanness of our gold surfaces under ambient conditions (see Fig. 2 (a)).

Right after the image of clean Au surfaces was obtained, we used two methods for the disposal of the molecules over the surfaces obtaining for both identical results. First, we used the drop-casting method in which the solvent was deposited onto the surface and dried under argon gas. Thereafter, the sample was dried-out down to 10^{-3} mbar of pressure. The second method is based in ambient temperature thermal evaporation, where the gold substrates were held above the solvent surface (non-

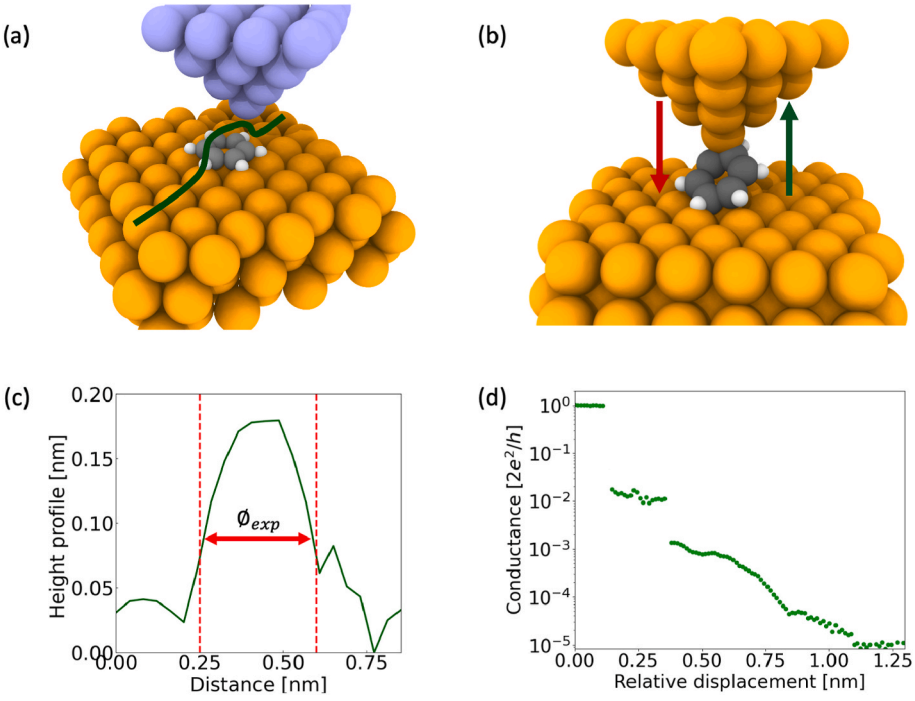

Fig. 1. Schematic illustration of (a) STM and (b) STM-BJ set up. Yellow and purple spheres correspond to the electrode atoms, Au and Pt-Ir respectively. Benzene is represented with gray and white spheres, as C and H atoms respectively. (c) Height profile of a single benzene molecule. Red dashed lines indicate the width at mid-height of the height profile measured in Fig. S1 from sup. inf. (d) Evolution of conductance while breaking a benzene molecular junction. (For interpretation of the references to color in this figure legend, the reader is referred to the Web version of this article.)

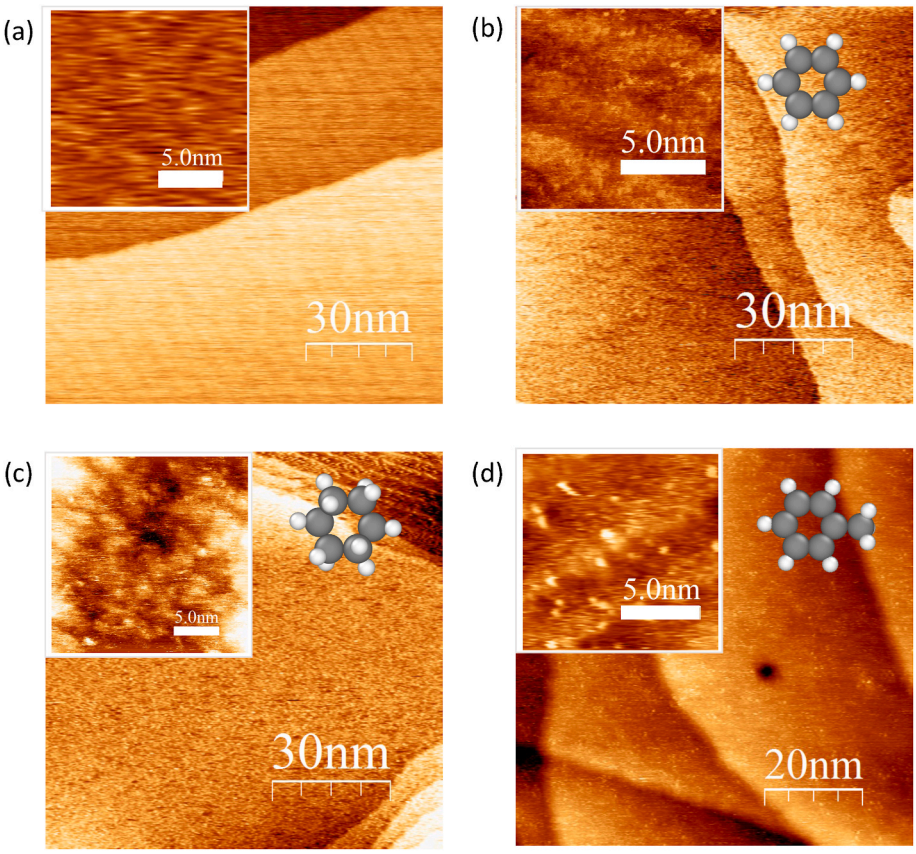

Fig. 2. Scanning Tunnelling Microscope images of a physisorbed molecular layer on Au(111) (a) clean gold surface (b) benzene (c) cyclohexane (d) toluene. The STM images were performed using tunnelling currents in the range 0.1–1.0 nA, and a voltage difference in between tip and sample of about 0.3–1.0 V (details in sup. inf. section. (For interpretation of the references to color in this figure legend, the reader is referred to the Web version of this article.)

immersed) in a closed glass vial.

3. Results and discussion

It should be stressed that prior to the STM imaging of the surfaces, we made our best to evaporate the deposited molecules with the aid of argon gas blowing and vacuum. Our STM images following the procedure above are shown in Fig. 2. In our images the Au(111) terraces are still clearly visible indicating that our deposition procedure did not affect the quality of the gold surface. However, even after our efforts to remove the molecules, these decorate the gold surfaces through a reproducible molecular arrangement. In Fig. 2, STM topographic images show the presence of the three deposited molecules (b) benzene, (c) cyclohexane and (d) toluene, decorating the surfaces. Following the procedure of preparation and evaporation the topographic images show a high reproducibility. The reported results were obtained on the first day of scanning although similar results could be obtained on the second day.

Topographic images were acquired using a bias voltage between 0.3 and 0.7 V applied to the tip in a current constant mode of 0.1–1.0 nA (details in sup. inf. section). The inserts in Fig. 2 show zooms of regions where it is feasible to distinguish single molecules as bright dots. Although atomic resolution of the molecules is not possible due to the molecular thermal diffusion at ambient conditions, the high molecular coverage of the molecules over the surface restricts enough the movement of the molecules allowing us to obtain details of the molecular sizes as shown in Fig. 1(c). The possible interactions among the molecules and molecules-substrate (mainly van der Waals forces) can affect the geometry binding, albeit when working with planar molecules as we are studying here, the most probable spatial distribution of the molecules would be parallel to the substrate. For the reasons depicted above, the ring structure of the three molecules cannot be differentiated in the images, but the measurement of the molecular diameter is feasible. This procedure is described in the work of Baciu et al. [31] by taking the width at mid-height of the height profile of the molecules (Fig. 1 (c)). The measured sizes are compare with the literature values which are in accordance with them as collected in Table 1.

Our results clearly confirm the presence of the three organic solvents on the gold surface but only in the thin layer, as the Au(111) terraces are still visible. This indicates that, as we expected, the very first layers of the three organic solvents under study are firmly physisorbed to the gold surface.

The existence of strong binding forces in between the gold surface and the studied molecules opens the possibility of forming single metal-molecule-metal junction without the need of the presence of anchoring groups.

For studying the formation of molecular bridges of our three organic solvents we use an improved STM-BJ experimental setup under room conditions. This technique [35,36] is, with the Mechanically Controllable Break Junction [37] (MCBJ), one of the most common approaches used for studying the electronic transport in atomic [38,39] or molecular

Table 1
First column indicates the molecule, second column shows the mean value and standard deviation of our diameter measured experimentally (φ_{exp}) and, third column offers the diameter found in the literature (φ_{lit}).

Molecule	φ_{exp} [nm]	φ_{lit} [nm]
Benzene	0.34 ± 0.01	0.28 [32], 0.25 [33], 0.38 [34]
Cyclohexane	0.40 ± 0.02	0.31 [32], 0.49 [34]
Toluene	0.38 ± 0.01	0.42 [32]

conductors [6]. In the STM-BJ approach, the two electrodes can move one respect to the other, as depicted in Fig. 1(b). They are firstly crashed and then, gently retracted allowing for the formation of the molecular bridge (more details about STM-BJ experimental setup in sup. inf. section). During this procedure, the conductance of the molecular bridge is recorded at a constant bias voltage (in our case ~100 mV) and conductance vs. electrode-displacement curves are built, the so-called traces of conductance. Our results and analysis are based in the traces of conductance during rupture of the bridge (rupture traces) as shown in Fig. 1 panel (d).

In the rupture traces, we first observe the breaking of the metallic bridge formed in between the two electrodes in the range above 1 G_0. Below this breaking point, we enter into the tunneling regime of conductance which is originated from the presence of tunnel barriers when the electrodes are separated, and can be described by the exponential decay. The presence of a molecular bridge will be shown as a plateau in conductance vs. relative displacement, instead of the exponential decrease. The transmission of the conductance channel through the molecule will depend on many factors including the alignment of the molecular levels to the Fermi energy of the electrodes in such a way that the conductance will get close to G_0 for the fully opened channel, otherwise it would decrease exponentially as the energy of the molecular orbitals of the molecular bridge move away from the Fermi energy of the electrodes and the electrodes are being separated.

We have characterized the Au-Molecule-Au bridges for the three molecules under study. For this experiments we prepared the electrodes to assure the cleanness in break-junctions experiments (see sup. inf. section). Once we guaranteed the absence of contaminants, we introduce the target molecules directly on the surface. Thus, when performing the experiment for each molecule, we can observe electrode-molecule junctions plateaus in the rupture traces, as shown in Fig. 1 (d). Our rupture traces are composed by 1024 points of conductance versus piezo displacement, values that were acquired by a NI-PCI-2689 with a sample rate about 21000 Samples/s. From these rupture traces we can construct conductance histograms, which reveals in a peak shape the most frequent values of conductance obtained. These histograms can be expressed in linear scale to obtain information for values bigger than 1 G_0 or in semi-logarithmic scale to highlight the values below the quantum of conductance. Every different molecule and their characteristic orientations respect to the electrodes can be distinguishable in the histograms as visible peaks, converting the histogram in a unique fingerprint of every different single metal-molecule-metal junction [40].

In our study, we can distinguish the traces where a molecule was present from those were only traces of gold single-atom contact, followed by a tunneling current from the electrodes. The main difference in between these two would be the formation of conductance plateaus or not. In Table 2 is reported the actual relative traces which contain the electrodes data and the molecular contributions separated by data selection. For this purpose, we define it as a criterion for considering clean gold when the conductance trace do not have significant counts under 0.8 G_0. In the literature the characteristic gold peak is in the range between 0.8 and 1.2 G_0 [41,42].

Table 2 shows that benzene is present in 50% of our junctions, whereas this percentage increases up to 80% and 70% in cyclohexane and toluene respectively. These percentages of molecular presence are assumed to depend on the density of molecules above the electrode surface. We first hypothesized that the low amount of benzene's traces could be explained for being the one with the lowest boiling point of the three [43]. However, the cyclohexane whose boiling point is 0.6 °C higher than the benzene, shows the highest value of presence of the molecular bridge, on the other hand, the boiling point for toluene is 30 °C higher than cyclohexane, where the molecular presence is smaller. Another possibility is to look at the strength of the activation energy for desorption [44], but this hypothesis fails because the most highest percentage of molecular bridge (cyclohexane) has the lowest value of energy desorption. Other possible factor can be attributed to the geometries including the flatness of the molecules. The presence of a molecular bridge will depend on different factors such as, the degree of coverage of the different molecules on the surfaces, their diffusion over the surface or the strength of the Au-Molecule binding [44]. However, the ratio of presence of the solvent on the surface is an open question, and maybe a combination of these different factors could explain the differences ratios of Table 2.

Table 2
Percentage of data traces with and without the presence of a molecular bridge.

	Benzene	Cyclohexane	Toluene
Gold contact	50%	20%	30%
Molecular bridge	50%	80%	70%

For the traces in which the molecules were anchored we constructed three different histograms that constitute the fingerprint of the molecules, as stated above, and can give us important information on the overlap of the molecular orbitals to electrons at the Fermi energy at the metallic electrodes. Fig. 3 displays a collection of histograms built from a set of thousands of rupture traces as previously defined. For the statistical analyses, around 3000 traces of clean gold has been considered for reference. On the other hand, the molecular contribution histograms were constructed from over 10000 traces for the different molecular junctions. These histograms are represented in Fig. 3.

In order to analyze the statistical distribution, we fit the data to Gaussian functions $\left(f(x) = \sum_{i=1}^{N} A\, e^{-(x-\mu)^2/2\sigma^2}\right)$, were μ corresponds to the peak of the most probable conductance. The typical histogram of gold is described in Fig. S2 of the supporting information[†] where the histogram of clean gold is shown. In Fig. 3 panels (a1),(b1) and (c1) compare the typical histogram of clean gold (black line) with the histogram of the respective molecular contribution (shaded gray area). The most probable values of conductance are collected in Tables 3 and 4 as a function of the regime under study. It is important to note that below the quantum of conductance, we plot the logarithmic data and also, a log scale representation was used to emphasize the peaks.

The molecular contribution is observed in the linear and logarithmic data representation in Fig. 3. Our histograms are normalized to the gold contact at $1G_0$. Therefore the strength of the molecular peak can be compared to the amount of bare gold traces and shows to be higher for the case of cyclohexane and toluene.

Linear histograms (Fig. 3 (a1), (b1) and (c1)) show a slight shift of the peak related to the atomic contact of gold at the quantum of conductance (black line). To unveil its origin, we use a two Gaussian fit in this region (Fig. 3 (a2), (b2) and (c2)) following the work of Sabater et al. [42]. In their manuscript, they characterize the monomeric, dimeric and double contact contributions for gold, silver and cooper histograms of conductance through the fitting of at least three Gaussians. Note that a monomer means the presence of solely one atom attached to the electrodes and a dimer is built by two atoms in line between the electrodes. This procedure allows us to disentangled our peak as the sum of two main contributions related to the formation of monomers (Fit #1) and dimers (Fit #2) with the molecular contribution. The fitting parameters are collected in Table 3.

One should notice that, although the conductance distribution for the dimeric contacts is unaltered with the presence of the molecules, there is an increase in the width of the distributions for the monomeric contacts when the molecule is present. This shift may be related to a contribution of the molecules to the conductance. Also, there is a widening in the peak around 0.8 G_0 in the linear scale, though it is not appreciated for benzene.

Now, if we focus in the peaks coming from the molecular bridges below the quantum of conductance, we distinguish for each molecule, three main distributions shown with different colored areas (see Fig. 3 panels (a3), (b3) and (c3)). It is quite remarkable to notice the strong similarity in between the distributions that may come from the

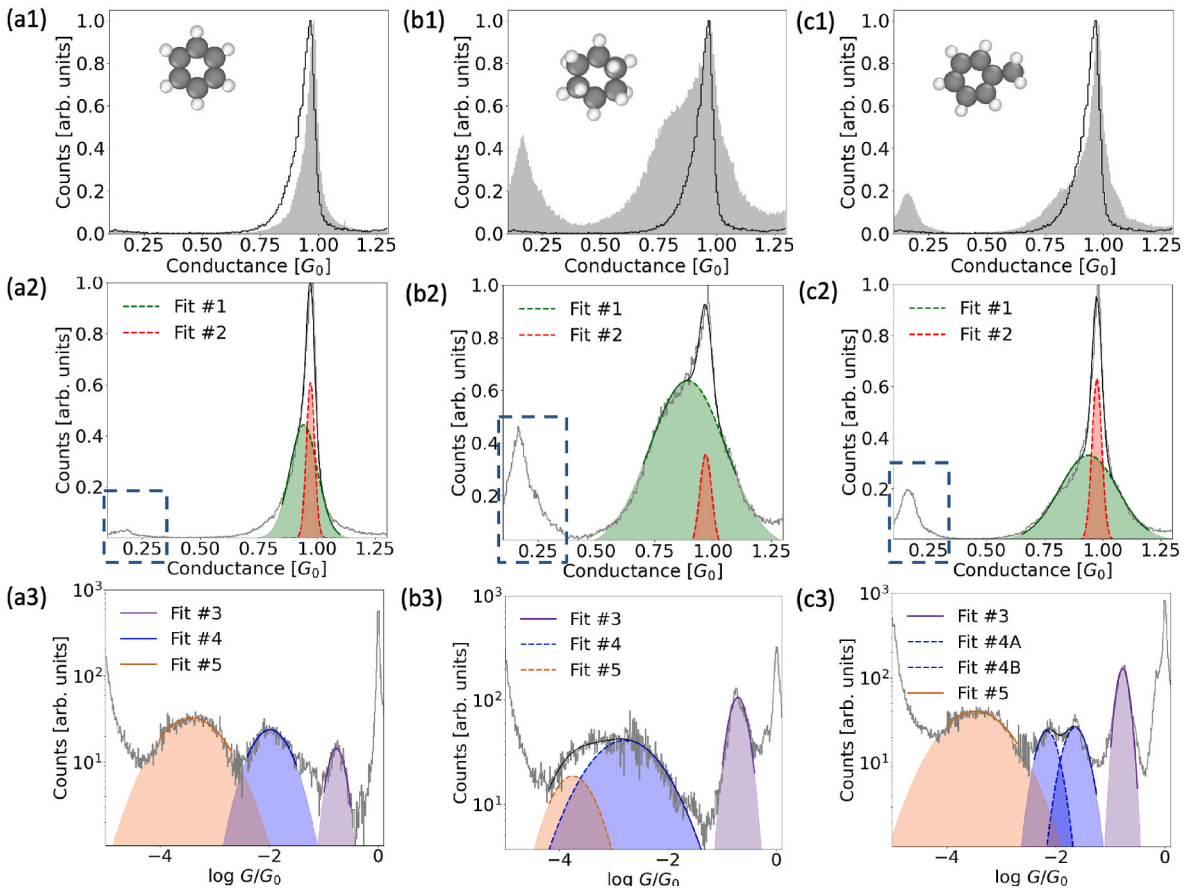

Fig. 3. Conductance histograms (normalized to the maximum value) of the three solvents deposited on gold. First (a1-a3), second (b1-b3) and third (c1-c3) columns show the results of benzene, cyclohexane and toluene respectively. First row presents a comparison between the clean histogram of gold (black line) with the histogram of conductance obtained when molecules are inserted (shaded gray area). In the second row the conductance of a single-atom gold contact is analyzed by Gaussian fits. Green and red shaded areas may be related to the monomeric and dimeric configurations of gold summed with the molecular contributions (Fit #1 and #2). The molecular contribution is indicated by the rectangle in dash blue. To resolve the molecular peaks at lower conductance value, the histograms are presented in logarithmic scale in the third row. Purple, blue and brown measurements come from the molecules when they adopt different attachments to the electrodes while stretching the junction (Fit #3, #4 and #5). Here the black lines represent the sum of two Gaussian contributions which fits with the data trend. Each shaded colored area is supposed to be related to different binding configurations. (For interpretation of the references to color in this figure legend, the reader is referred to the Web version of this article.)

Table 3
Gaussian fits to the conductance close to 1 G_0 for pure gold and the molecular contribution. Color code of the letters matches to the colored areas used in panels (a2), (b2) and (c2) Fig. 3.

	Pure Gold $\mu_i \pm \sigma_i$	Benzene $\mu_i \pm \sigma_i$	Cyclohexane $\mu_i \pm \sigma_i$	Toluene $\mu_i \pm \sigma_i$
Monomer	0.92 ± 0.06	0.94 ± 0.07	0.89 ± 0.16	0.94 ± 0.12
Dimer	0.96 ± 0.02	0.97 ± 0.02	0.97 ± 0.03	0.98 ± 0.02

Table 4
Most probable conductance values (G) obtained from Gaussian fits under the quantum of conductance regime for solvent molecules. Color code of the letters matches to the colored areas used in Fig. 3 (a3), (b3) and (c3).

	$G_{Fit\ \#3}$ [G_0]	$G_{Fit\ \#4}$ [G_0]	$G_{Fit\ \#5}$ [G_0]
Pure Gold	Featureless		
Benzene	$1.6 \cdot 10^{-1}$	$1.1 \cdot 10^{-2}$	$3.8 \cdot 10^{-4}$
Cyclohexane	$1.9 \cdot 10^{-1}$	$1.5 \cdot 10^{-3}$	$1.7 \cdot 10^{-4}$
Toluene	$1.7 \cdot 10^{-1}$	$2.3 \cdot 10^{-2}$	$3.4 \cdot 10^{-4}$
		$7.1 \cdot 10^{-3}$	

similarity, also, in between the three molecules. Benzene and cyclohexane are prototypes of an aromatic (delocalized π electrons in the molecular plane) and aliphatic molecule (localized sigma electrons), while toluene is a mixed aromatic-aliphatic molecule sharing features from both. Therefore one should expect differences in between their conductances to be subtle, similar for toluene and benzene and lower for cyclohexane. Our data fits only logarithm scale, therefore these fitting values are logarithmic (fitted conductance values (μ) along their deviations (σ) are collected in Table S1 sup. inf. section). In Table 4, we summarize the fitting parameter for the different conductance peaks as a function of G_0.

The highest peak in the range (1.6–1.9) $\cdot 10^{-1}$ G_0 is almost identical for the three molecules. As these conductances are so similar, the delocalized electrons present in benzene or toluene should not play any role. Therefore, the most probable origin for this peak should be related to the presence of the molecular ring being perpendicular to the direction of the electrodes. We should point out that this result for benzene is in good agreement with the work by Tal's group [45] at low-temperature using silver electrodes. The second peak is the one showing the main differences in between the three molecules, differences which follows our initial guess stated above. In this case, the conductance is similar for benzene ($1.1 \cdot 10^{-2}$ G_0) and toluene ((0.7–2.3) $\cdot 10^{-2}$ G_0) but much lower and difficult to disentangle from the third for the case of cyclohexane ($1.5 \cdot 10^{-3}$ G_0). It is also remarkable to observe a

splitting of the second peak for the case of toluene most likely coming from the presence of the methyl group. Other peaks at lower values may appear from molecular staking [46].

To get more insight, we analyzed the overall shape of the evolution of the conductance traces. For this we study the average trace for each molecule that can be constructed as a 2D density plot as shown in Fig. 4. For making this plot we took into consideration only the traces with molecular contribution, which are traces with plateaus below the atomic conductance. The point at which conductance takes the value of, at least, the one of the atomic contact of gold ($G < 1.1\ G_0$), is taken as the origin for the electrodes relative displacement, and then these are added up to form the 2D density plot.

The first of the density plots (a) shows that, for the case of clean gold electrodes at ambient conditions, it is feature-less from about $5 \cdot 10^{-4}\ G_0$ to the region of the atomic contacts at about G_0. Below $10^{-4}\ G_0$ we can observe a signal coming from the tunneling current between electrodes that fade to the electrical noise of our amplifier when the electrodes are separated about 1.0 nm. We should notice that the color scale is logarithmic to make noticeable even individual events.

In these representations the contribution of the molecules is highlighted allowing the different details of the various geometrical configurations of the molecular bridges to be examined. The most important information given by this representation is the overall length and shape of the conductance plateaus for the different shapes for the molecular bridge. It is remarkable that the main differences observed are in the second peak contributions ($\sim 10^{-2}\ G_0$), especially in cyclohexane.

In Fig. 4 we observe two features that are coincident for the three studied molecules. First, the plateaus at about $10^{-1}\ G_0$ are plateaus remaining quite constant in value while stretched and the length of the plateaus is similar (slightly shorter) to the one related to the one-atom bridge between electrodes (traces at $\sim 1\ G_0$). This indicates that in this configuration the bind of the molecules to the electrodes is similar (slightly lower) to the one of the one atom. As we concluded from the histograms before, all the facts imply that these traces are most likely related to the plane of molecules being perpendicular to the direction of the contact (see Fig. 5).

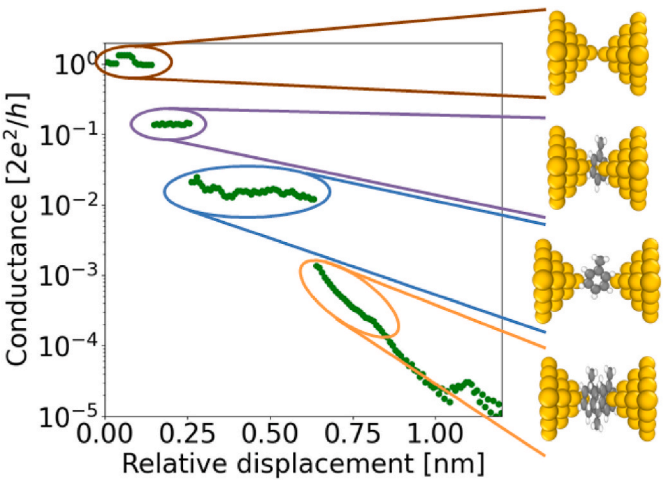

Fig. 5. A toluene rupture trace with the presence of different plateaus related to different atomic and molecular geometrical configurations. Atomic gold sized-contact, perpendicular, parallel and staked molecular bridges are illustrated from top to the bottom, respectively. Color code of circles and lines matches to the colored areas used in panels (a3), (b3) and (c3) Fig. 3. (For interpretation of the references to color in this figure legend, the reader is referred to the Web version of this article.)

The second set of traces shared by the three molecules is the one with a mean conductance of about $10^{-3}\ G_0$. In this occasion the plateaus are longer and decrease over 1–2 orders of magnitude in conductance. This fact implies a weak bonding of the molecules to the electrodes. This configuration is also shown to happen, on average, ~0.2 nm after the gold contact was formed, normally even after the presence of a previous molecular junction. The conductance plateaus in this region are also much longer than the ones related to the atomic contact. The three features above, long plateaus after the atomic and molecular contacts and strong decrease of conductance while stretching, indicate a weak junction most likely related to the conductance over a number of staked

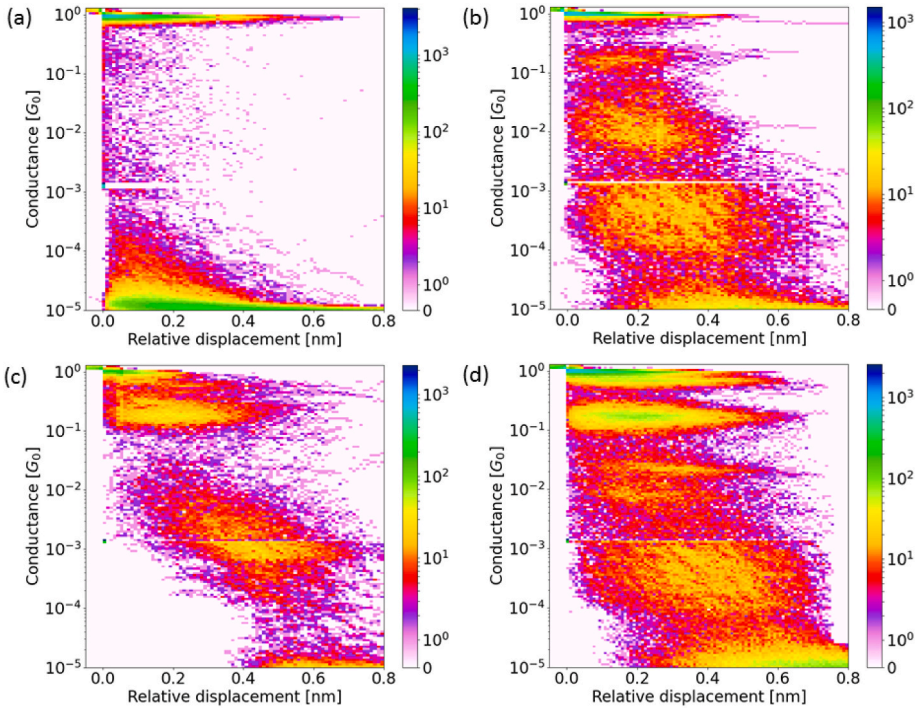

Fig. 4. Density plots according to the conductance histograms of (a) clean gold, (b) benzene, (c) cyclohexane and (d) toluene. (For interpretation of the references to color in this figure legend, the reader is referred to the Web version of this article.)

molecules [46] (see Fig. 5). The fact of a thin molecular layer over the metallic surface may limit the number of staked molecules and may be the reason why there is a lower value for that peak at about $3 \cdot 10^{-4}\ G_0$.

Where the differences in between the three molecules unveil is on the set of traces that for the case of benzene or toluene can be found at about $10^{-2}\ G_0$. In this case, we find again a set of traces with plateaus of constant conductance and with plateau lengths similar to the ones related to the one-atom bridge between electrodes. As we previously discussed these facts indicate a well bonded molecular bridge. The variations observed in this peak for the different molecules is an indication of the role of the extended molecular π orbital of the molecules in the case of benzene and toluene. Therefore this configuration should correspond to the molecular ring being parallel to the direction of the electrodes (see Fig. 5). In fact, for the case of cyclohexane, although we could fit the histogram in the area of $10^{-3}\ G_0$ to two Gaussian curves, we find difficult to find signatures of this configuration in the density plot. It is possible that we are not detecting the signatures of this geometrical configuration for cyclohexane due to the lack of an extended molecular orbital in this molecule. Finally, we should notice that in the case of toluene this peak is split, most likely, due to the presence of the methyl group which breaks its symmetry. This can be taken as a fingerprint to distinguish in between aliphatic and aromatic series of molecules.

4. Conclusions

In summary, we have proven the presence of an adsorbed molecular layer over a gold surface, of the three organic solvents, benzene, cyclohexane and toluene, at ambient conditions. The strength of the adsorbed molecular layer is tight enough to the electrodes to permit the characterization of their role in molecular electronics.

The presence of the molecules on Au(111) surfaces has been clearly identified through STM topographic images. We have been able to distinguish individual molecules of sizes between 3 and 4 Å. The observation of thin molecular films decorating the gold substrates, supports our conclusion that our measurements are related to stable single-molecules junctions. The study of the conductance characteristics of the molecular junctions has allowed us to identify the different conductive states of single molecules attached to gold electrodes and to establish their characteristic conductance signature.

Our results imply the existence of an important contribution of the studied molecules on surfaces at ambient conditions. Their influence should be not neglected when these are being used for the preparation of experiments at ambient conditions as we have proven the difficulty of their removal through common preparation procedures and their role in different experiments in molecular electronics.

Author information

All authors have given approval to the final version of the manuscript.

CRediT authorship contribution statement

Tamara de Ara: Data curation, Methodology, Software, Formal analysis, Investigation, Validation, Writing – review & editing. **Carlos Sabater:** Conceptualization, Writing – original draft, Writing – review & editing, Supervision, Resources, Visualization, Project administration, Funding acquisition. **Carla Borja-Espinosa:** Data curation, Software, Investigation. **Patricia Ferrer-Alcaraz:** Data curation, Software, Investigation. **Bianca C. Baciu:** Investigation, Methodology, Writing – review & editing. **Albert Guijarro:** Resources, Writing – review & editing, Funding acquisition. **Carlos Untiedt:** Resources, Writing – review & editing, Supervision, Project administration, Funding acquisition.

Declaration of competing interest

The authors declare that they have no known competing financial interests or personal relationships that could have appeared to influence the work reported in this paper.

Data availability

Data will be made available on request.

Acknowledgements

This work was supported by the Spanish Government through MAT2016-78625-C2 and PID2019-109539 GB-C41, and also supported by the Generalitat Valenciana through PROMETEO/2017/139, PROMETEO/2021/017, and CDEIGENT/2018/028. We want to thank Prof. N. Agraït for his fruitful tips and advices in the use of combined I-V converters.

Appendix A. Supplementary data

Supplementary data to this article can be found online at https://doi.org/10.1016/j.matchemphys.2022.126645.

References

[1] C.A. Martin, D. Ding, J.K. Sørensen, T. Bjørnholm, J.M. van Ruitenbeek, H.S.J. van der Zant, Fullerene-based anchoring groups for molecular electronics, J. Appl. Comput. Sci. 130 (2008) 13198–13199.
[2] D. Boer, M. Coenen, M. Maas, T. Peters, O. Shklyarevskii, J. Elemans, A. Rowan, S. Speller, Electron transport through co studied by gold break-junctions in nonpolar liquids, J. Phys. Chem. C 113 (2009).
[3] K. Luka-Guth, S. Hambsch, A. Bloch, P. Ehrenreich, B.M. Briechle, F. Kilibarda, T. Sendler, D. Sysoiev, T. Huhn, A. Erbe, E. Scheer, Role of solvents in the electronic transport properties of single-molecule junctions, Beilstein J. Nanotechnol. 7 (2016) 1055–1067.
[4] D. Xiang, X. Wang, C. Jia, T. Lee, X. Guo, Molecular-scale electronics: from concept to function, Chem. Rev. 116 (2016) 4318–4440.
[5] R.H.M. Smit, Y. Noat, C. Untiedt, N.D. Lang, M.C. van Hemert, J.M. van Ruitenbeek, Measurement of the conductance of a hydrogen molecule, Nature 419 (2002) 906–909.
[6] S. Aradhya, L. Venkataraman, Single-molecule junctions beyond electronic transport, Nat. Nanotechnol. 8 (2013) 399–410.
[7] F. Evers, R. Korytár, S. Tewari, J.M. van Ruitenbeek, Advances and challenges in single-molecule electron transport, Rev. Mod. Phys. 92 (2020), 035001.
[8] J.C. Cuevas, E. Scheer, Molecular Electronics, second ed., WORLD SCIENTIFIC, 2017.
[9] C.J. Lambert, Quantum Transport in Nanostructures and Molecules, IOP Publishing, 2021, pp. 2053–2563.
[10] O. Tal, M. Kiguchi, W.H.A. Thijssen, D. Djukic, C. Untiedt, R.H.M. Smit, J.M. van Ruitenbeek, Molecular signature of highly conductive metal-molecule-metal junctions, Phys. Rev. B 80 (2009), 085427.
[11] J.M. Bopp, S. Tewari, C. Sabater, J.M. van Ruitenbeek, Inhomogeneous broadening of the conductance histograms for molecular junctions, Low Temp. Phys. 43 (2017) 905–909.
[12] M. Valášek, K. Edelmann, L. Gerhard, O. Fuhr, M. Lukas, M. Mayor, Synthesis of molecular tripods based on a rigid 9,9′-spirobifluorene scaffold, J. Org. Chem. 79 (2014) 7342–7357.
[13] L. Gerhard, K. Edelmann, J. Homberg, M. Valášek, S.G. Bahoosh, M. Lukas, F. Pauly, M. Mayor, W. Wulfhekel, An electrically actuated molecular toggle switch, Nat. Commun. 8 (2017), 14672.
[14] B. Xu, N.J. Tao, Measurement of single-molecule resistance by repeated formation of molecular junctions, Science 301 (2003) 1221–1223.
[15] D. Stefani, C. Guo, L. Ornago, D. Cabosart, M. El Abbassi, M. Sheves, D. Cahen, H.S. J. van der Zant, Conformation-dependent charge transport through short peptides, Nanoscale 13 (2021) 3002–3009.
[16] Y. Liu, L. Ornago, M. Carlotti, Y. Ai, M. El Abbassi, S. Soni, A. Asyuda, M. Zharnikov, H.S.J. van der Zant, R.C. Chiechi, Intermolecular effects on tunneling through acenes in large-area and single-molecule junctions, J. Phys. Chem. C 124 (2020) 22776–22783.
[17] S. Fujii, M. Iwane, S. Furukawa, T. Tada, T. Nishino, M. Saito, M. Kiguchi, Hybrid molecular junctions using au s and au π bindings, J. Phys. Chem. C 124 (2020) 9261–9268.
[18] J. Zheng, J. Liu, Y. Zhuo, R. Li, X. Jin, Y. Yang, Z.-B. Chen, J. Shi, Z. Xiao, W. Hong, Z.-q. Tian, Electrical and sers detection of disulfide-mediated dimerization in single-molecule benzene-1,4-dithiol junctions, Chem. Sci. 9 (2018) 5033–5038.

[19] F. Chen, X. Li, J. Hihath, Z. Huang, N. Tao, Effect of anchoring groups on single-molecule conductance: comparative study of thiol-, amine-, and carboxylic-acid-terminated molecules, J. Appl. Comput. Sci. 128 (2006) 15874–15881.
[20] L.A. Zotti, T. Kirchner, J.-C. Cuevas, F. Pauly, T. Huhn, E. Scheer, A. Erbe, Revealing the role of anchoring groups in the electrical conduction through single-molecule junctions, Small 6 (2010) 1529–1535.
[21] L. Venkataraman, J. Klare, I. Tam, C. Nuckolls, M. Hybertsen, M. Steigerwald, Single-molecule circuits with well-defined molecular conductance, Nano Lett. 6 (2006) 458–462.
[22] M.A. Reed, C. Zhou, C.J. Muller, T.P. Burgin, J.M. Tour, Conductance of a molecular junction, Science 278 (1997) 252–254.
[23] J. Ulrich, D. Esrail, W. Pontius, L. Venkataraman, D. Millar, L.H. Doerrer, Variability of conductance in molecular junctions, J. Phys. Chem. B 110 (2006) 2462–2466.
[24] C. Li, I. Pobelov, T. Wandlowski, A. Bagrets, A. Arnold, F. Evers, Charge transport in single au — alkanedithiol — au junctions: coordination geometries and conformational degrees of freedom, J. Appl. Comput. Sci. 130 (2008) 318–326.
[25] M. Kiguchi, O. Tal, S. Wohlthat, F. Pauly, M. Krieger, D. Djukic, J.C. Cuevas, J. M. van Ruitenbeek, Highly conductive molecular junctions based on direct binding of benzene to platinum electrodes, Phys. Rev. Lett. 101 (2008), 046801.
[26] T. Yelin, R. Vardimon, N. Kuritz, R. Korytár, A. Bagrets, F. Evers, L. Kronik, O. Tal, Atomically wired molecular junctions: connecting a single organic molecule by chains of metal atoms, Nano Lett. 13 (2013) 1956–1961.
[27] G. Binnig, H. Rohrer, C. Gerber, E. Weibel, Surface studies by scanning tunneling microscopy, Phys. Rev. Lett. 49 (1982) 57–61.
[28] Goodfellow, Description and publicity. Metal trading supplier. https://www.goodfellow.com.
[29] Arrandee, Description and publicity. Metal trading supplier. https://www.arrandee.com.
[30] C. Wöll, S. Chiang, R.J. Wilson, P.H. Lippel, Determination of atom positions at stacking-fault dislocations on au(111) by scanning tunneling microscopy, Phys. Rev. B 39 (1989) 7988–7991.
[31] B.C. Baciu, T. de Ara, C. Sabater, C. Untiedt, A. Guijarro, Helical nanostructures for organic electronics: the role of topological sulfur in ad hoc synthesized dithia[7] helicenes studied in the solid state and on a gold surface, Nanoscale Adv. 2 (2020) 1921–1926.
[32] Andrew Gibert, Description and publicity IQmol open-source molecular editor and visualization package. https://www.iqmol.org.
[33] R. Whiddington Lonsdale, The structure of the benzene ring in $C_6(CH_3)_6$, Proc. Roy. Soc. Lond. 123 (1997).
[34] H. Madani, A. silvestre albero, M. Biggs, F. Rodriguez-Reinoso, P. Pendleton, Immersion calorimetry: molecular packing effects in micropores, ChemPhysChem 16 (2015).
[35] J.I. Pascual, J. Méndez, J. Gómez-Herrero, A.M. Baró, N. García, V.T. Binh, Quantum contact in gold nanostructures by scanning tunneling microscopy, Phys. Rev. Lett. 71 (1993) 1852–1855.
[36] N. Agraït, J.G. Rodrigo, S. Vieira, Conductance steps and quantization in atomic-size contacts, Phys. Rev. B 47 (1993) 12345–12348.
[37] J.M. Krans, C.J. Muller, I.K. Yanson, T.C.M. Govaert, R. Hesper, J.M. van Ruitenbeek, One-atom point contacts, Phys. Rev. B 48 (1993), 14721.
[38] J. Krans, J. van Ruitenbeek, L. de Jongh, Atomic structure and quantized conductance in metal point contacts, Phys. B Condens. Matter 218 (1996) 228.
[39] N. Agraït, A.L. Yeyati, J.M. Van Ruitenbeek, Quantum properties of atomic-sized conductors, Phys. Rep. 377 (2003) 81–279.
[40] A. Mishchenko, D. Vonlanthen, V. Meded, M. Bürkle, C. Li, I.V. Pobelov, A. Bagrets, J.K. Viljas, F. Pauly, F. Evers, M. Mayor, T. Wandlowski, Influence of conformation on conductance of biphenyl-dithiol single-molecule contacts, Nano Lett. 10 (2010) 156–163.
[41] C. Sabater, M. Caturla, J. Palacios, C. Untiedt, Understanding the structure of the first atomic contact in gold, Nanoscale Res. Lett. 8 (2013) 257.
[42] C. Sabater, W. Dednam, M.R. Calvo, M.A. Fernández, C. Untiedt, M.J. Caturla, Role of first-neighbor geometry in the electronic and mechanical properties of atomic contacts, Phys. Rev. B 97 (2018), 075418.
[43] P. Linstrom, in: W. Mallard (Ed.), NIST Chemistry WebBook, NIST Standard Reference Database Number 69, National Institute of Standards and Technology, 2017. https://webbook.nist.gov/chemistry. (Accessed 17 March 2021).
[44] S.M. Wetterer, D.J. Lavrich, T. Cummings, S.L. Bernasek, G. Scoles, Energetics and kinetics of the physisorption of hydrocarbons on Au(111), J. Phys. Chem. B 102 (1998) 9266–9275.
[45] T. Yelin, R. Korytár, N. Sukenik, R. Vardimon, B. Kumar, C. Nuckolls, F. Evers, O. Tal, Conductance saturation in a series of highly transmitting molecular junctions, Nat. Mater. 15 (2016) 444–449.
[46] S.T. Schneebeli, M. Kamenetska, Z. Cheng, R. Skouta, R.A. Friesner, L. Venkataraman, R. Breslow, Single molecule conductance through multiple $\pi - \pi$ stacked benzene rings determined with direct electrode to benzene ring connections, J. Appl. Comput. Sci. 133 (2011) 2136–2139.